Simulation of CO_2 concentrations at Tsukuba tall tower using WRF-CO_2 tracer transport model

Srabanti Ballav[1,4,*], Prabir K Patra[2], Yousuke Sawa[3], Hidekazu Matsueda[3], Ahoro Adachi[3], Shigeru Onogi[3], Masayuki Takigawa[2] and Utpal K De[1]

[1]*School of Environmental Studies, Jadavpur University, Kolkata 700 032, India.*
[2]*Department of Environmental Geochemical Cycle Research, JAMSTEC, Yokohama 236-0001, Japan.*
[3]*Meteorological Research Institute, Tsukuba, Ibaraki 305-0052, Japan.*
[4]*Present address: Aryabhatta Research Institute of Observational Sciences (ARIES), Manora Peak, Nainital 263 002, Uttrakhand, India.*
[*]*Corresponding author. e-mail: srabanti_ballav@yahoo.co.in*

Simulation of carbon dioxide (CO_2) at hourly/weekly intervals and fine vertical resolution at the continental or coastal sites is challenging because of coarse horizontal resolution of global transport models. Here the regional Weather Research and Forecasting (WRF) model coupled with atmospheric chemistry is adopted for simulating atmospheric CO_2 (hereinafter WRF-CO_2) in nonreactive chemical tracer mode. Model results at horizontal resolution of 27 × 27 km and 31 vertical levels are compared with hourly CO_2 measurements from Tsukuba, Japan (36.05°N, 140.13°E) at tower heights of 25 and 200 m for the entire year 2002. Using the wind rose analysis, we find that the fossil fuel emission signal from the megacity Tokyo dominates the diurnal, synoptic and seasonal variations observed at Tsukuba. Contribution of terrestrial biosphere fluxes is of secondary importance for CO_2 concentration variability. The phase of synoptic scale variability in CO_2 at both heights are remarkably well simulated the observed data (correlation coefficient >0.70) for the entire year. The simulations of monthly mean diurnal cycles are in better agreement with the measurements at lower height compared to that at the upper height. The modelled vertical CO_2 gradients are generally greater than the observed vertical gradient. Sensitivity studies show that the simulation of observed vertical gradient can be improved by increasing the number of vertical levels from 31 in the model WRF to 37 (4 below 200 m) and using the Mellor–Yamada–Janjic planetary boundary scheme. These results have large implications for improving transport model simulation of CO_2 over the continental sites.

1. Introduction

Simulation of high-frequency measurements of CO_2 at hourly/weekly timescales around a complex terrain or diverse ecosystem is challenging for the coarse resolution global chemistry-transport models (CTMs), typically with horizontal resolutions of 1°× 1° and only a few vertical layers in the first 1 km from the earth's surface. Further, the spatial and temporal resolutions of surface fluxes used in global CTMs are coarser than that is required for realistic representation of the continental or coastal measurement sites. Thus, understanding of the limitations of forward transport model simulation of CO_2 at hourly to synoptic timescales, has attracted considerable interest in recent times (e.g., Law *et al.* 2008; Patra *et al.* 2008). Because the model–observation data mismatch is one of the main

Keywords. WRF-CO_2 model; Tsukuba tall tower; model–observation comparison; synoptic variation; diurnal cycle.

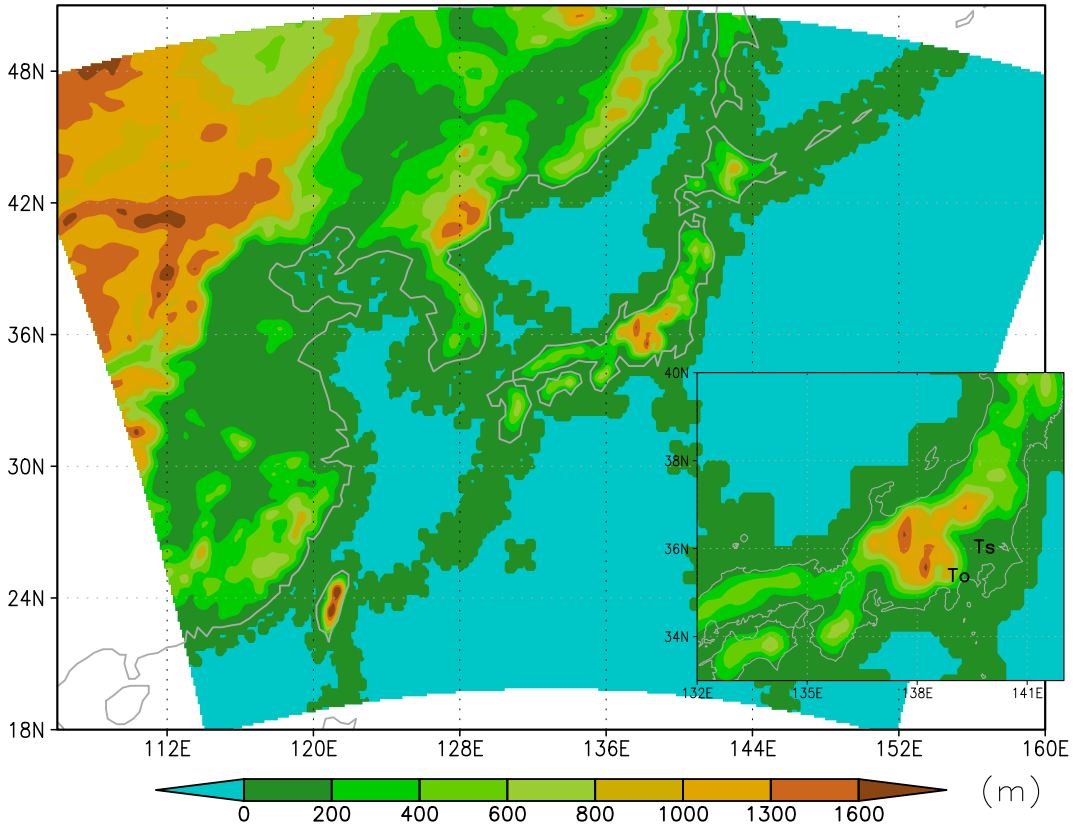

Figure 1. The model domain with terrain height in meter (colour bar used) is represented. The CO_2 observation station at Tsukuba (marked by Ts) and megacity Tokyo (marked by To) are shown in the inset.

factors involved in the inverse modelling of sources and sinks at the earth's surface, setting up of the best possible *a priori* concentration simulation system is critical for the success of an inverse modelling system (Tolk *et al.* 2011; Peylin *et al.* 2011). The quality of forward simulations depends to a large extent on our ability to represent the heterogeneity of surface fluxes and model transport behaviour around the site (Tolk *et al.* 2008). Recent studies using regional chemistry models have successfully relaxed the limitation in model horizontal resolution and account for the heterogeneity in the surface fluxes, and thus resolving the fine structures in CO_2 concentration variation over the Western European continents (e.g., Sarrat *et al.* 2009; Pillai *et al.* 2011; Vogel *et al.* 2013), American continents (Freitas *et al.* 2009; Corbin *et al.* 2010; Moreira *et al.* 2013), East Asian region (Ballav *et al.* 2012) and Mediterranean Sea (Palmiéri *et al.* 2015).

CO_2 measurements at tall towers (200–400 m height from surface) over land show large changes in concentrations along the vertical as strong signals from net uptake (dominated by photosynthesis) during the summer days, net release (dominated by respiration) during the night and anthropogenic emission, are mixed and propagated into the atmosphere through the planetary boundary layer (PBL) (e.g., Bakwin *et al.* 1995; Denning *et al.* 1995; Haszpra *et al.* 2012). The photosynthesis/respiration and the mixing height (MH) of trace gases are the function of solar radiation and are correlated to each other (Seibert *et al.* 1998). The synthetic experiment of minimizing MH error by Kretschmer *et al.* (2012) found ∼25–30% uncertainty in simulated MH during day time over land. Gerbig *et al.* (2008) showed uncertainty in MH produces 3 ppm error on forward transport model which inter-generates 30% uncertainty in estimated CO_2 flux. Using optimized MH (Kretschmer *et al.* 2014) in CO_2 transport simulation, the model bias reduces 5–45% in day time and 60–90% in night time. Pillai *et al.* (2011) carried out their study at a tower over Ochsenkopf mountain top in Germany surrounded by valleys and hills, and also used a regional model (Ahmadov *et al.* 2007) to validate their observed data. The mountain valley circulations and terrain induced up-down slope circulations greatly influence the diurnal variation of CO_2 concentration at Ochsenkopf. Smallman *et al.* (2014) investigated the contribution of ecosystem-specific net CO_2 uptake/release tracers to the tall tower signal in Scotland by simulating the coupled numerical weather model WRF-SPA (Weather Research Forecasting model and Soil–Plant–Atmospheric Model) for 3 years. Miles *et al.* (2012) considered CO_2 concentration variation

at nine-towers regional networks during North American Carbon Program's Mid-Continent Intensive in 2007–2009. They could explain the monthly concentration variation at the tower sites on the basis of the influence of different biomes like corn, soy, grass and other forest vegetation over the region. The monthly averaged gradients in CO_2 over the central USA region were tied to regional patterns in net ecosystem exchange. Ballav *et al.* (2012) found that the daily scale variations in CO_2 at several sites in the East Asia region are governed by local environmental condition, local weather and large scale weather patterns.

We are extending the study by Ballav *et al.* (2012) to a tower site at Tsukuba, located 60 km northeast of central Tokyo, Japan, which may be categorized as a semi-urban site. To understand the orography of the area surrounding the tower, a local map is given with terrain height (figure 1). Almost 60% of the land in Japan are national parks or reserved forests and about 10% of the whole country population resides in and around Tokyo, leading to a complex mixture of strong CO_2 emissions/sinks, in and around Tsukuba. Prompted by these challenges, we have attempted to simulate CO_2 concentrations over the East Asia region using the WRF-CO_2 model developed at Jadavpur University, India in collaboration with Research Institute of Global Change/Japan Agency for Marine-Earth Science and Technology (RIGC/JAMSTEC) (Ballav *et al.* 2012). CO_2 and meteorological measurements at the site are being made by Meteorological Research Institute (MRI), Tsukuba, Japan. Our aim is to simulate the vertical profile of CO_2 at the Tsukuba tall tower. This is to test the limitations of a regional transport model in more complex environment unlike the previous analyses being carried out for remote locations with diverse environmental characteristics (Ballav *et al.* 2012). In particular, a more complex issue, i.e., the vertical propagation of CO_2 concentration is addressed here. Apart from analysis of the year-long control simulations, sensitivity runs by changing the vertical resolution of the model and using a different PBL parameterization scheme have been performed towards improving the model transport.

2. Descriptions of WRF-CO_2 model and Tsukuba tower measurements

The descriptions of Weather Research and Forecasting model's dynamical core coupled with atmospheric chemistry (WRF-Chem) formulation can be found in Grell *et al.* (2005). The fundamental setup of the WRF modelling domain and parameterization selections are essentially similar to those described earlier (Takigawa *et al.* 2007; Ballav *et al.* 2012). As stated in the previous section, the tracer transport component for CO_2 simulations has been newly developed by two research groups. The domain of WRF-CO_2 extends from ∼101°E in the west to ∼165°E in the east, and ∼18° to ∼51°N along the south–north, with the center at 133°E, 35°N in the Lambert Conformal coordinate system. The horizontal resolution of the domain and the vertical levels remain the same as in the previous study (Ballav *et al.* 2012). Tsukuba is nearly 5 km from a nearest grid point of our model.

Emissions due to fossil fuel over the entire domain have been utilized from TransCom3 experiment (Law *et al.* 2008; Patra *et al.* 2008; referred to as FS) or Emission Database for Global Atmospheric Research (EDGAR; Olivier and Berdowski 2001). The archive of EDGAR (http://edgar.jre.ec.europa.eu/archived_datasets.php) version 3.2 has 1°× 1° resolution, which is coarser compared to the horizontal resolution of WRF-CO_2 model.

The Carnegie–Ames–Stanford Approach (CASA) model simulated 3-hourly mean data (being referred as CH) for terrestrial biological activity, are used at 1°× 1° horizontal resolution, which is again sufficiently poor, if we consider the land use pattern (Olsen and Randerson 2004 and references therein). The oceanic exchanges (OC) at 4°×5° resolution are taken from Takahashi *et al.* (2002). All these fluxes are converted to WRF model grid using 5-point stencils before the transport simulation experiment. It should be pointed out that poor resolution flux data is used in the present work, in comparison with the resolution of the regional model (27×27 km). In fact, we have fossil fuel flux data of much higher resolution (0.1°× 0.1°) from EDGAR4.0, but not used here because terrestrial ecosystem fluxes with matching resolution are not available.

The initial and boundary conditions (IC/BCs) for CO_2 concentration are used from the global atmospheric general circulation model (AGCM)-based Chemistry-Transport Model (ACTM) (Patra *et al.* 2008; Law *et al.* 2008) and the IC/BCs for meteorological parameters are used from the National Centers for Environmental Prediction (NCEP) final analysis data (Ballav *et al.* 2012).

Tsukuba tower has six levels (i.e., 10, 25, 50, 100, 150, 200 m) for observation of meteorological parameters, but CO_2 concentration is available at three levels only, i.e., at 1.5, 25 and 200 m, respectively. However, 1.5 m observation cannot be used because of coarse resolution of the model. Concentration data at each level was acquired at 18 min interval (1 min for signal integration and 5 min for switching and replacing the gas in the sample line at each tower level) and 1-hourly averaged values are calculated from 2–4 data points at each level.

Table 1. *Pearson moment correlation coefficients of simulated CO_2 concentrations and various tracer components like fossil fuel emission, biogenic and oceanic with the observed daily variability at the Tsukuba tower. The normalized standard deviations (NSDs) are given within parenthesis. NSD is defined as model standard deviation to observed standard deviation. Model offset for FS+CH+OC tracer is 375 ppm, and bias is calculated as average of model-observation. In the first column left height represents for observation and the right one for model.*

Height (m)	FS+CH+OC	FS	CH	OC	Bias
All months of 2002					
25–45	0.72 (0.69)	0.73 (0.70)	–0.09 (0.14)	0.00 (0.04)	–0.07
200–120	0.71 (0.57)	0.76 (0.56)	–0.12 (0.21)	0.07 (0.06)	–0.37
200–220	0.57 (0.41)	0.69 (0.37)	–0.13 (0.21)	0.07 (0.06)	–2.62
January–March 2002					
25–45	0.70 (0.77)	0.74 (0.77)	–0.20 (0.14)	–0.11 (0.04)	–0.08
200–120	0.63 (0.66)	0.78 (0.63)	–0.29 (0.21)	–0.10 (0.06)	–0.48
200–220	0.45 (0.45)	0.73 (0.39)	–0.33 (0.22)	–0.10 (0.06)	–2.98
April–June 2002					
25–45	0.78 (0.78)	0.78 (0.77)	–0.02 (0.20)	0.29 (0.05)	1.31
200–120	0.76 (0.54)	0.73 (0.53)	–0.02 (0.21)	0.30 (0.06)	–0.78
200–220	0.62 (0.42)	0.64 (0.38)	–0.03 (0.20)	0.31 (0.06)	–2.41
July–September 2002					
25–45	0.77 (0.72)	0.77 (0.73)	–0.05 (0.15)	0.07 (0.02)	–0.30
200–120	0.77 (0.53)	0.78 (0.53)	–0.01 (0.19)	0.16 (0.03)	–1.80
200–220	0.71 (0.41)	0.75 (0.38)	0.05 (0.19)	0.17 (0.03)	–3.79
October–December 2002					
25–45	0.65 (0.59)	0.67 (0.60)	–0.13 (0.11)	–0.07 (0.04)	–1.27
200–120	0.66 (0.57)	0.77 (0.58)	–0.26 (0.22)	–0.05 (0.09)	1.61
200–220	0.37 (0.34)	0.65 (0.32)	–0.34 (0.22)	–0.05 (0.09)	–1.29

The basement of the tower usually remains covered with dense grass, easily growing in thin organic clay soil, and the tower is surrounded by deciduous and coniferous trees (Inoue and Matsueda 2001). The temperature drops to 3°C in January and the average surface temperature of the site area increases to 23°C in August. On the other hand, the monthly mean precipitation amount exceeds 100 mm from April to October.

The four lowermost η levels near the ground are at 1.0, 0.993, 0.980 and 0.966. The model gives output of CO_2 concentration at the staggered levels located at the middle of two consecutive η levels. Here, CO_2 concentration outputs at the first and second staggered levels (around 45 and 120 m heights respectively) are matched with 25 and 200 m vertical height observation, though the next staggered level at 220 m is closer to 200 m. The reason for such choice is to have better matching of the concentrations between 120 m of model height and 200 m of observed height. This clearly points to poor vertical propagation of CO_2 concentration in the model. When comparison is made between 220 m of model height and 200 m of observed height, correlation coefficient (CC), normalized standard deviation (NSD) and diurnal amplitude show significant deviations from the observations (table 1), which is consistent with the observations made in TransCom3 continuous analysis (Law *et al.* 2008). The model is run from 1 January, 2002 (0000 UT) to 31 December, 2002 (2400 UT), while first 5 days of the simulation are considered as model spin-up and left out of the statistical analysis.

3. Results and discussion

3.1 *Seasonality of meteorology at Tsukuba tower site*

The observed wind rose patterns at 25 and 200 m of the tower levels for four seasons of the year 2002 are plotted in figure 2. In general, the horizontal winds are more organized at 200 m, which is located above the canopy height top, if compared with those near the ground at 25 m. As Tokyo is located south to southwest (S–SW) of Tsukuba, southwesterly to southerly winds are expected to transport very strong anthropogenic emission signals (high concentration) from Tokyo area to Tsukuba, northwesterly (NW) wind will bring signals from highly variable terrestrial ecosystem exchange, and easterly wind will bring background air representing the Pacific Ocean.

Let us now describe the transport situation from Tokyo region in different seasons. The westerly

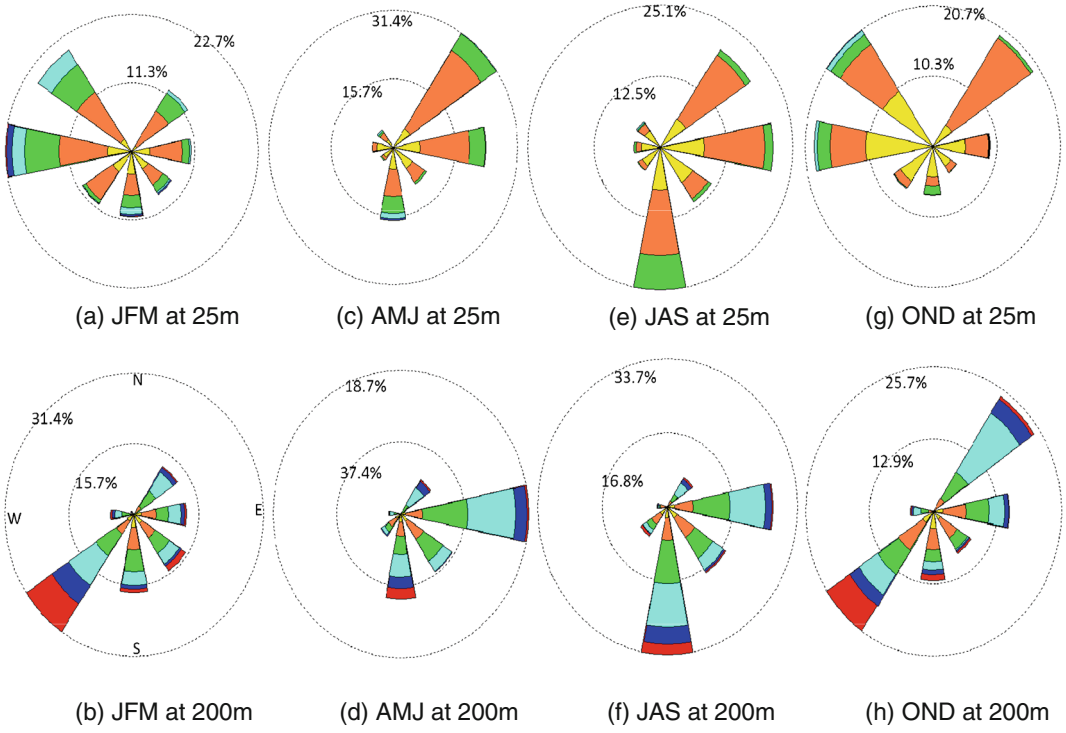

Figure 2. Observed wind distributions at Tsukuba are provided for different seasons of the year 2002. January–March (JFM), April–June (AMJ), July–September (JAS) and October–December (OND) are the four seasons. While (**a**, **c**, **e** and **g**) stand for 25 m height, (**b**, **d**, **f** and **h**) for 200 m height. Wind speed is given by different colour codes, yellow (0–1.5), orange (1.5–3.0), green (3.0–5.0), cyan (5.0–8.0), blue (8.0–10.0) and red >10.0. All measurements are made in m/s. The bigger circle provides the maximum frequency of occurrence in time.

wind at 25 m height is most dominant during winter season (January–March), and SW or southerly winds are infrequent. The SW wind is most frequent at 200 m, along with significant southerly and small frequency of westerly wind (figure 2b). During the spring season (April–June) (figure 2c, d), southerly winds are sometime observed both at 25 and 200 m heights along with small frequencies of SW or westerly. During the summer season (July–September; figure 2e, f), winds are dominantly southerly. Westerlies are sufficiently dominant at 25 m height (figure 2g) in the autumn season (October–December), whereas SW wind dominates at 200 m height (figure 2h).

3.2 *Day–night variation of model CO_2 in association with wind circulation*

The general features in CO_2 concentration distribution and wind pattern of WRF-CO_2 model at 45 m vertical level with the Tsukuba tower site at the center are depicted in different panels of figure 3 for a day in winter and two days in summer respectively. While the first panel stands for 15 January, 2002, those in the second and third panels are for 29 June, 2002 and 31 July, 2002 respectively. For the summer season, we choose two days with different features. While, 29 June, 2002 falls within a period when the CO_2 concentration was low over a stretch of some days; 31 July, 2002 is a particular day of the year at Tsukuba when the observed concentration rose to an unusually high value of above 480 ppm at 0300 Japan Standard Time (JST=UT+09 hours). This is incidentally the highest concentration observed at Tsukuba during the summer season of 2002. Each panel on the left column is for 0300 JST and that on the right column is for 1500 JST.

The emissions from Tokyo due to fossil fuel burning are seen as hotspot in figure 3(a, b) with CO_2 concentrations exceeding 400 ppm, while the background concentration over the other parts of the country and the sea on either side of the Japan Islands are in the range of 370–380 ppm. During winter (January), the terrestrial biosphere acts as net source of CO_2, both during day and night, and the boundary layer depth does not change much, giving rise to relatively uniform concentration distribution. The wind pattern has a front at the north-west corner of the domain and a high pressure zone on the east of the landmass at 0300 JST on 15 January, 2002. The wind is strong on the south of the front, which travels southward at least by 3° in the next 12 hrs (i.e., at 1500 JST). The winds around Tsukuba are more organized and stronger in the afternoon.

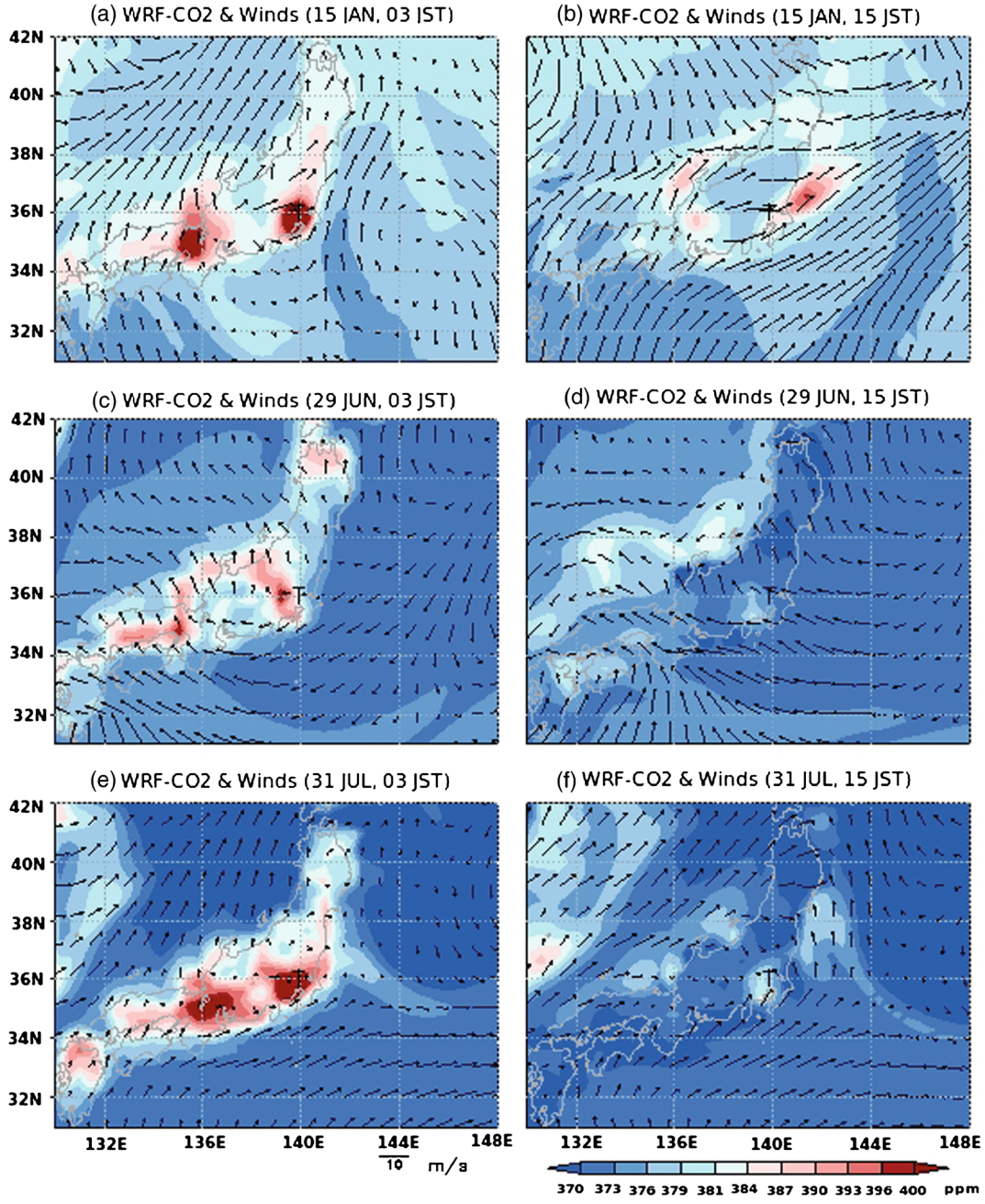

Figure 3. Latitude–longitude distributions of simulated WRF-CO_2 (FS+CH+OC) concentration and wind are provided at the model level 1, with the Tsukuba Tower site at the center (marked by T). Typical day- and night-time conditions are presented for a chosen date during the boreal winter (15 January 2002) and 2 days in summer season (29 June and 31 July, 2002).

Next, we consider the CO_2 concentration and wind pattern distribution over the domain on 29 June, 2002 (figure 3 c, d). In summer, the biological fluxes consist of overall strong drawdown of carbon during day (1500 JST) and dominant heterotrophic respiration during the night (0300 JST), and in its wake, day time concentration at level 1 of the model gets largely depleted, whereas the night time concentration are elevated over the land areas. At night time, the fossil emission from the city hotspots also remain trapped in the stable boundary layer which has much lower depth, to give larger concentration. The wind pattern during the day and night does not undergo much change.

The general concentration pattern over day and night respectively does not differ much on 31 July, 2002 (figure 3 e, f) from those of 29 June, 2002, except that the high concentration prevails over large part of the Japanese landmass at 0300 JST. Southwesterly (SW) wind prevails over the southern half of the country, though the modelled winds are lower than 8 m/s. In fact, the wind pattern does

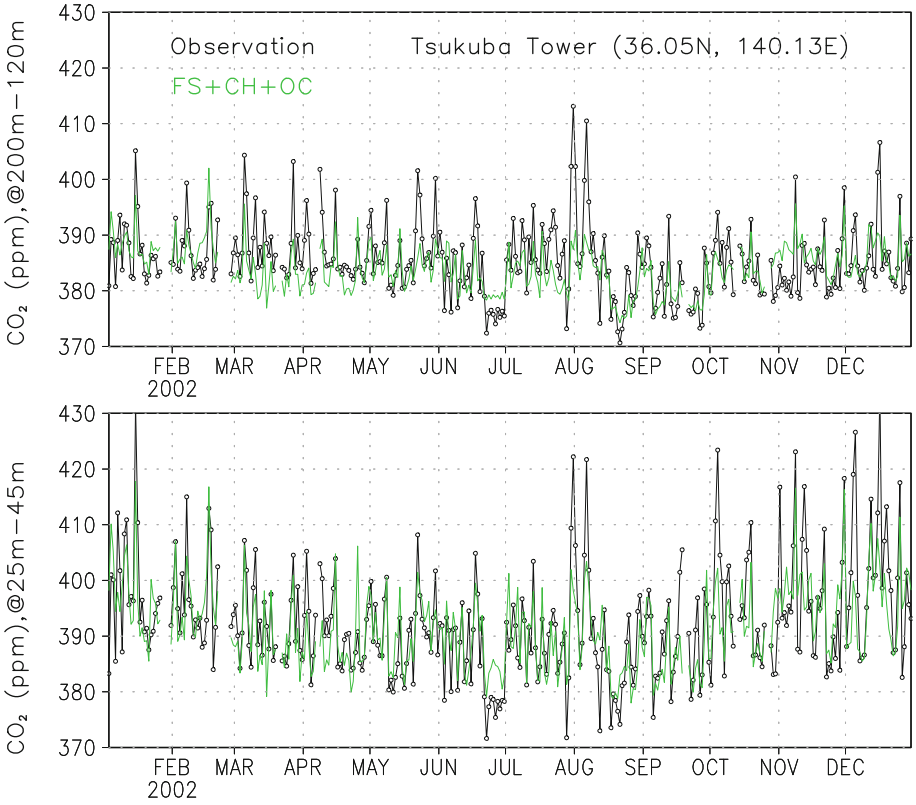

Figure 4. Time series of measured (at 25 and 200 m tower heights) and WRF-CO_2 simulated concentrations (at 45 and 120 m heights). The bottom figure stands for the lower height and the top one is for the upper height.

not undergo much change during day and night, except in the northeast part of the domain.

3.3 *Comparison of observed and simulated CO_2 concentration at Tsukuba tower site*

The observed and simulated CO_2 concentrations, averaged at daily interval, are presented in figure 4 for the entire year for the two heights of the Tsukuba tower. Simulated concentrations are considered for the tracer combination of FS+CH+OC. The observed concentration is low during July to September in general due to strong drawdown of CO_2 by terrestrial vegetation during boreal summer. The patterns of variation for measured as well as modelled concentration are not much different at two heights. This is reflected by high value of CC between the two products at each season (table 1).

The annual as well as seasonal correlations at different matching heights are presented in table 1. The CCs are evaluated for deseasonalized time series obtained using a filtering technique (Nakazawa *et al.* 1997). Correlations of individual tracers, FS, CH and OC, with the observed concentration, are also included in the table. CC of all tracers combined in table 1 are found to be high (CC $\geq$ 0.71, when the entire year is considered), if the matching of 220 m of model height with 200 m of observed height is not considered. In the second case, it falls to $\geq$0.57. The correlations are 1% significant following Student t-test (i.e., holds in 99% cases) with at least 85 data points. This shows that the model can capture the phase of the concentration variations statistically significant with the present choice of comparison and control simulation case. The summer-time CCs are, in general, higher compared to winter-time CCs, as the daily fluctuations in winter concentration are high, which cannot be captured by the model (may be noted in figure 4).

Table 1 shows that the correlation of observed CO_2 with FS tracer component only, has a high value, almost comparable to that of the tracer combination FS+CH+OC. This clearly points to the dominance of fossil emission transport in CO_2 concentration variations at the Tsukuba tower site. Obviously, the negative value of CC for CH tracer lowers the same for the combination. This will be further discussed in section 3.5 from the viewpoint of the diurnal cycle.

It may be mentioned here that in case of global ACTM simulations, the synoptic or shorter scale variations do not show good correspondence with the measured variability as expected, because Tokyo and Tsukuba cities fall within one horizontal

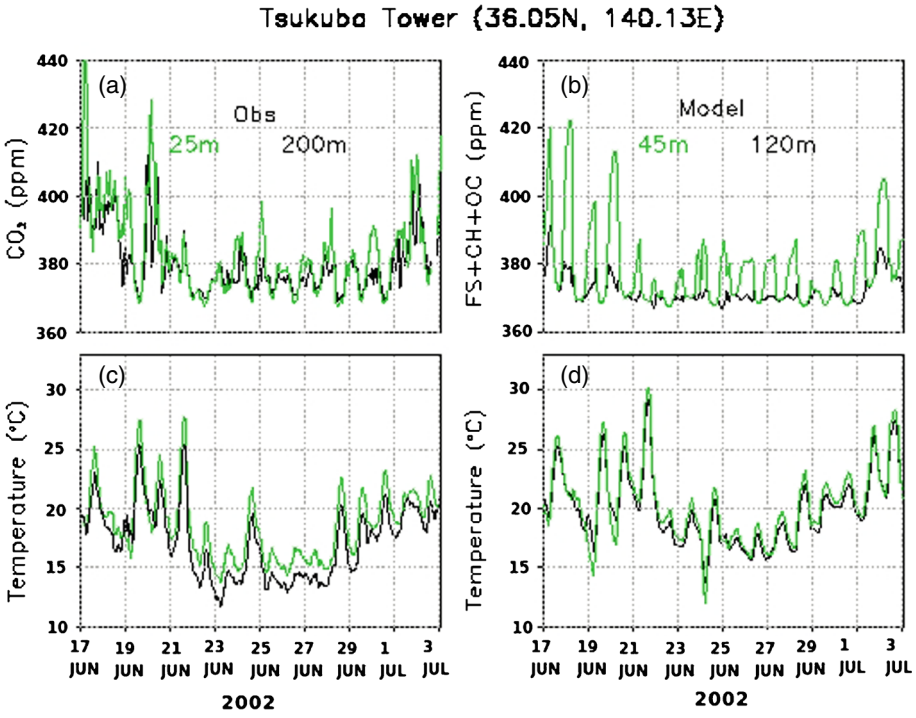

Figure 5. Observed and simulated parameters during a low CO_2 concentration episode from 0000 JST, 17 June, 2002 to 0000 JST, 3 July, 2002. Panels (**a**, **b**) stand for CO_2 concentration in ppm, (**c**, **d**) for temperature in °C. While the left figures (a, c) provide the observed quantities, the right figures (b, d) provide simulated values. On the left panels (a, c), two observation heights of 25 and 200 m and on right panels (b, d) two simulated heights of 45 and 120 m are considered.

grid cell of most global models. Higher resolution of the regional model can separate the two locations at two completely different grid cells that brings out different output characteristics. Thus, a finer model resolution improves the simulation. Further improvement is possible if input flux data also have matching resolution with that of the WRF-CO_2 model and the WRF nested grid is implemented for zooming over smaller region, say only over the Kanto plain (Takigawa *et al.* 2007). We have chosen to run the model for one full year, and because of coarse resolution of input fluxes, the nesting capability is not implemented in the present study.

On the other hand, the NSDs, which are the ratio of the model standard deviation to the observed standard deviation, are always less than unity. So, the model gives less fluctuation compared to what is observed. NSDs are higher at 25 m height compared to that at 200 m height, though the difference appreciably reduces in the months of October–December. During these months, the vertical mixing is much better as will be shown in section 3.4; this apparently leads to closer NSD value at the two heights. Comparison of the model concentration at 220 m and observed concentration at 200 m shows that NSD value has sharp fall. This again points to poor vertical propagation of the concentration up to 220 m height.

We first adjust an offset for the model CO_2 results at 45 m with observed concentration at 25 m for the entire 2002 and then calculate bias in simulated concentrations with respect to observations. The offsets are maintained at constant value for all model levels with tracer combination. If the model bias is evaluated taking the difference of average of model to observed concentration, analysis of average model bias at different heights (table 1) shows that negative bias increase with height if the entire year is considered. Results for the winter, spring and summer seasons are consistent with those for the entire year average. The model-observation bias is positive for 120 m model *vs.* 200 m observation in autumn, but the biases for 45 and 220 m models are consistent if an offset of about –1.27 ppm is ignored or the offsets are corrected for different seasons separately. Because the terrestrial biosphere fluxes are not optimized for this study, the CO_2 seasonal cycle amplitudes are not very well compared with observed amplitude (ref. the biases for the lowermost layer for different seasons in table 1).

Figure 4 shows that the observed CO_2 concentration has low value from some hour of 20 June to 1 July, and it oscillates around 380 ppm. The concentration and temperature at the two heights during the period 0000 JST, 17 June –0000 JST, 3 July are shown for clarity in separate figures (figure 5a–d).

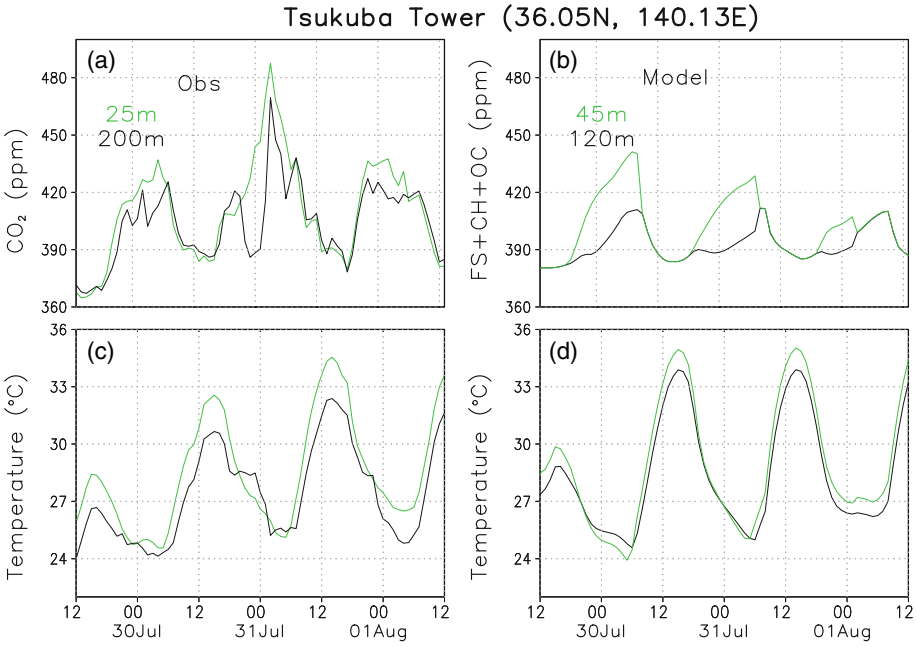

Figure 6. Observed and simulated parameters from 1200 JST, 29 July, 2002 to 1200 JST, 1 August, 2002 around a sharp concentration rise event. While panels (**a**, **b**) stand for CO_2 concentration in ppm, (**c**, **d**) for temperature in °C. Left figures (a, c) provide the observed quantities and the right figures (b, d) stand for simulation. In each figure, two heights are considered, i.e., 25 and 200 m for observation, and 45 and 120 m for model.

The diurnal variation was significantly less even at 25 m height and it was further less at 200 m height (figure 5a). The diurnal variation almost disappeared on 22–23 June at both the tower heights. During the entire period, the wind came mainly from the sea and this might be one of the important reasons for such a low concentration regime (the same may also be seen from figure 3c and d).

Apart from that, the observed vertical temperature gradient was considerably negative throughout this period, during day and night and many a time it was more than the adiabatic lapse rate (figure 5c), which resulted in thermal instability and it helped to reduce the lower level concentration to a significant extent. The observed concentration is close-by at both the levels following the usual characteristics of a convective mixed layer (figure 5a). There exists considerable model–observation mismatch in this case. Uncertainties associated with too strong FS emissions or too weak diurnal cycle in CH fluxes may contribute to this mismatch. The model can simulate well the low concentration of 380 ppm at 200 m height, but the simulated concentration has strong diurnal oscillation at 25 m height (figure 5b). The simulated temperatures (figure 5d) at the two levels show thermal stability, as the potential temperature shows a positive vertical gradient, which helps to enhance the simulated concentration at 25 m height.

Over the period of 17 June to 2 July, the CC between observed and simulated concentration is 0.72 for 25 m height and the same is 0.69 for 200 m height. On the other hand, NSD at two heights are starkly different. NSD at 25 m height is 0.92, which means that the model can simulate the concentration variability quite well. But, NSD at 200 m height drops to 0.46 only. This clearly points to lesser ability of the model in capturing the vertical propagation of the concentration.

Next, we consider an episode covering 72 hrs, i.e., from 1200 JST of 29 July to 1200 JST of 1 August. The observed concentration rose sharply above 480 ppm at 25 m height close to 0200 JST of 31 July (figure 6a). The concentration rose steadily from 390 ppm at 1500 JST of 30 July and after reaching the maximum, again fell steadily to slightly above 430 ppm at close to 0600 JST of 31 July. In fact, the highest observed concentration of the summer season occurred at the above-mentioned time. A number of factors possibly combined to create the situation. One important factor was the presence of significant temperature inversion (figure 6c) over some hours, i.e., from close to 2000 JST of 30 July to close to 0200 JST of 31 July. Inversion occurred again after 0300 JST almost for 3 hours. The observed wind speed at 25 m height was light throughout the 24-hr period, which helped to accumulate the CO_2 concentration in a stable atmosphere and the wind direction also caused transport from Tokyo region. The wind direction initially helped to raise the concentration, but a strong temperature inversion played a more important role. When inversion was ruptured at 0200

JST of 31 July, the concentration also started to fall. Such inversion was not observed on the other two days, so the concentration also did not rise to high value.

The observed concentration at 200 m height rose close to 470 ppm at the same time of 0200 JST of 31 July. The wind direction at 200 m height was mostly from the south over 24-hr period. Though the wind speed was comparatively stronger at this height, which might cause more mixing between the two heights, a strong transport possibly helped to bring sufficient CO_2 from the side of a big city. Another possibility might be local respiration from large canopies developed in summer.

During 1200 JST, 29 July–1200 JST, 1 August 2002, the simulated concentration (figure 6b) does not show such strong variability and we concentrate our discussion from 1200 JST of 30 July to 1200 JST of 31 July. During this period, the diurnal cycle shows a peak of nearly 30 ppm only at 25 m height. The peak has also a time shift to 0600 JST. The diurnal variability in concentration drops to only 20 ppm at 200 m height and time has a further shift at 0700 JST. The simulated temperature has inversion only from 0100 to 0500 JST. One important cause of this low diurnal cycle may be due to the wind direction being mostly from east side of south over the period and transport in this situation is not of much help for enhancing CO_2 concentration. It should be pointed out that, in coastal zones with high emission from nearby sources, a small shift in simulated wind direction towards the ocean side would cause large error in simulated concentration. Apart from that, biological activity is strong during summer, but a poor resolution of CH fluxes in the model may strongly affect the diurnal cycle.

3.4 *Vertical gradient of CO_2 concentration*

Figure 7(a) presents the average vertical profile of CO_2 concentration in four seasons (JFM: January–March, AMJ: April–June, JAS: July–September and OND: October–December), both for observed as well as simulated data. In case of observed data of CO_2 concentration, there are three levels at 1.5, 25 and 200 m; whereas we have model simulation output at 45, 120 and 220 m. On the other hand, there are six levels at 10, 25, 50, 100, 150 and 200 m for the observation of meteorological parameters. However, we show only the temperature vertical profiles in figure 7(b).

Figure 7(a) shows that the maximum gradient in observed concentration of CO_2 occurs in autumn (OND months) followed by winter (JFM). Minimum of observed concentration gradient occurs in AMJ, while those for the JAS months are slightly above. Model simulation follows exactly the same order. Strong vertical gradient for observed data in the layer of 25–1.5 m, cannot be compared with the model due to lack of vertical layers below 25 m. Further, the terrestrial biosphere fluxes from roots, stems and leaves should be appropriately distributed for below canopy top height. Presently no model, to the best of our knowledge, is capable of such handling of transport and fluxes within the canopy. The gradients in first simulated layer (120–45 m) are much less (may go down to 30% even) in comparison to those of the first observed layer of 25–1.5 m. A closer look at figure 7(a) shows that the gradient in OND is less in simulation compared to what is observed. But, the situation is reverse in the other three seasons. So, the model is giving higher vertical mixing in stable condition of OND.

Figure 7(b) shows the observed and simulated temperature profiles. In general, all simulated temperatures are close (within 1°C in most cases, and occasionally up to 2°C) to the observed ones for different seasons. In OND months, the observed temperature rises between the first level at 10 m and the last level at 200 m, apart from a strong temperature rise in 25–50 m layer (by 0.57°C). This is probably the main reason why the concentration gradient is highest in the lowest observed layer. This is expected in winter. The maximum stability during OND, gives maximum positive vertical concentration gradient. Heterotrophic respiration of the terrestrial biosphere is significant in this season during day and night, and this raises the surface concentration.

In the season of JFM, the observed temperature rise between the first and the last layers decreases compared to the previous case. So the overall stability diminishes, which leads to fall in positive vertical gradient of the concentration. In the case of other two seasons, the temperature systematically falls vertically and the rate increases from spring (AMJ) to summer (JAS). During these two seasons, concentration gradient is less in the upper layer.

For better understanding of the control of CO_2 fluxes and model transport on the CO_2 vertical profiles at the tower site, afternoon (referred as PM; 13–16 local time) (figure 7c, d) and late night (referred as AM; 01–04 local time) averages (figure 7e, f) are plotted for CO_2 (figure 7c, e) and temperature (figure 7d, f), respectively. Clearly the rise in CO_2 concentration from 1.5 to 25 m during the AMJ and JAS months in PM are caused by the photosynthetic uptake of carbon overtaking the fossil fuel emissions during the day. Since during the day the PBL is well mixed, as seen from unstable temperature profiles, the uptake signal is quickly transferred to higher altitudes and gets well mixed up to the tower top. During JFM

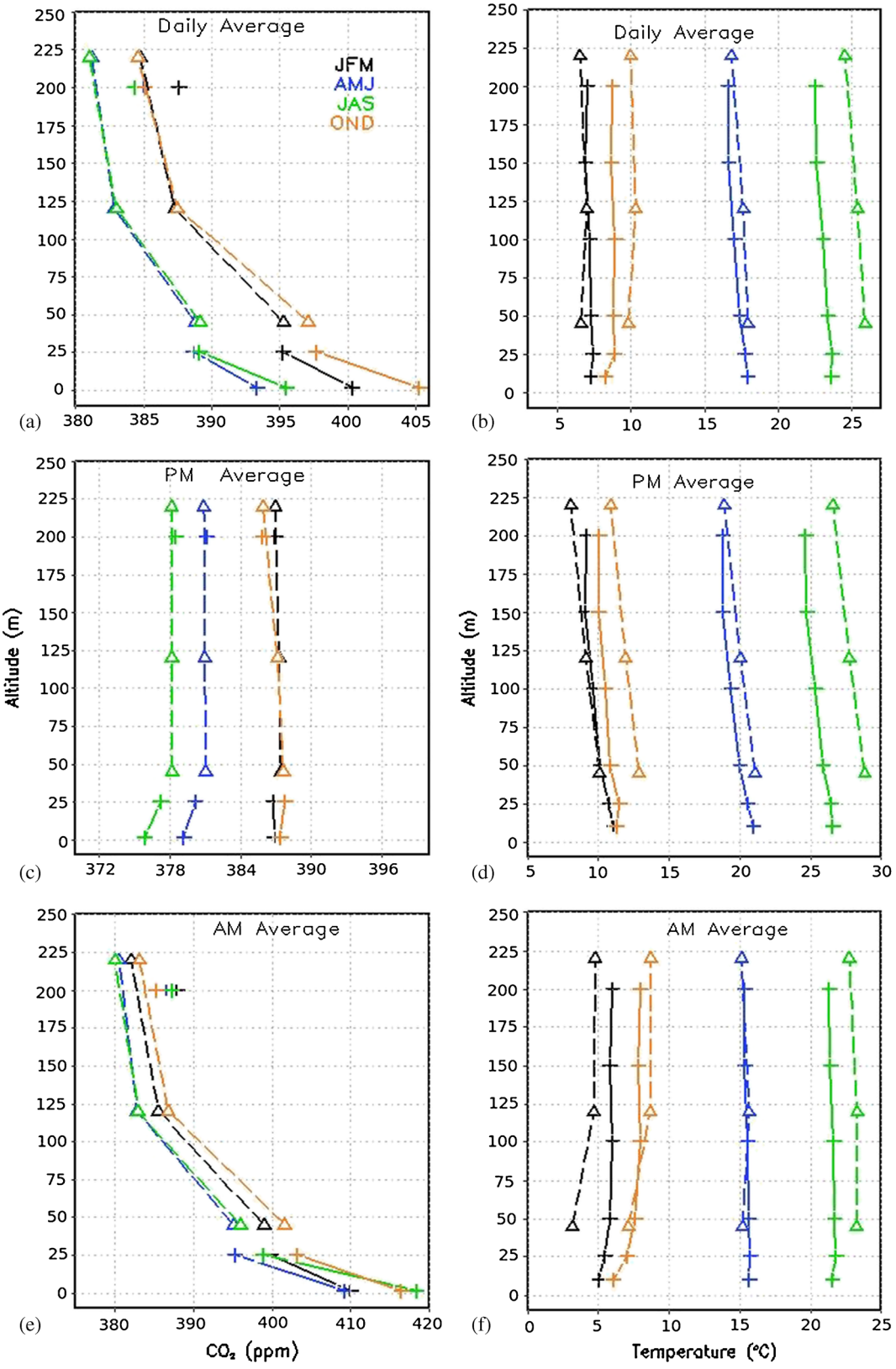

Figure 7. Comparisons of measured (plus symbols and solid lines) and simulated (open triangles and broken lines; tracer combination being FS+CH+OC) vertical profiles of CO_2 (left column) and temperature (right column) at Tsukuba, averaged over four seasons (JFM: January–March, AMJ: April–June, JAS: July–September, OND: October–December). While panels (**a**, **b**) stand for daily average data of CO_2 concentration and temperature, respectively; (**c**, **d**) for afternoon average (referred as PM; 13 to 16 local time) and (**e**, **f**) for late night average (referred as AM; 01 to 04 local time) of the same products. In panel (a), the observed concentrations at 200 m height have overlapped in AMJ and OND. In panel (e), the same at 200 m are approximately equal for JFM, AMJ and JAS.

and OND months, no significant vertical gradient is observed across all tower altitudes, indicating well mixed PBL condition, or the net photosynthetic/respiration flux signal is weak in these months. During the late night (AM), the vertical profile show very strong decrease in CO_2 concentrations with height in all seasons because of carbon release by heterotrophic respiration as well as the fossil fuel emissions. The model simulation is consistent with the situation in a stable atmosphere. The temperature profiles indicate the presence of weak to strong inversion layer in three seasons during the late night, except for the AMJ months. These features in CO_2 and temperature vertical profiles are captured to a large extent by the WRF-CO_2 model simulations.

3.5 *Monthly mean diurnal cycle of CO_2 concentration*

Observed as well as simulated (for FS + CH + OC flux combination) values of monthly mean diurnal cycle in different months at hourly interval are presented for two different heights in figure 8(a–d), respectively. Figures for the two tower heights are shown side by side. For the monthly average diurnal cycle, we have averaged the diurnal cycles calculated for each day at hourly interval within a given month.

The average diurnal cycle change at 25 m is significantly stronger compared to the corresponding value at 200 m height (consistent with the observation of Olsen and Randerson 2004). The maximum of the cycle in both the heights is observed in the early morning hours, when boundary layer is stable and shallow. The value drops around midday due to convection in the boundary layer and the rise starts again from early evening. The diurnal cycle amplitude is deeper in summer (>20 ppm) and much shallower in February–March (8–10 ppm). The model captures well, the night and early morning behaviours (figure 8c). Both, highest and lowest cycle amplitudes are observed in August–September. Highest diurnal cycle amplitude in model shifts to July and time is delayed by a couple of hours compared to the observation. Minimum in diurnal cycle amplitude is observed in August at around 1400 local time, but the minimum in simulated cycle occurs at 1600 local time. Strong change in diurnal cycle with vertical height before the mid-day is well captured by the model. Not so strong change in diurnal cycle with vertical height in the evening is also well captured by the model. In spite of these, deterioration in simulated value compared to observed magnitude in the upper level is conspicuous except during some months of winter. This, in general, points to poorer vertical propagation of the surface emission signals in WRF-CO_2 model.

When we compare figure 8(e) with 8(c) (both correspond to 45 m model height) and between figure 8(f) and 8(d) (for the model height of 120 m), we find that the major contribution to simulated CO_2 concentration comes from FS or fossil fuel burning/transport tracer component. Biogenic tracer component CH has also been presented at the two heights in figure 8(g and h). In general, contribution of CH tracer component to the diurnal cycle is much less compared to FS tracer component. But CH tracer gives significant emission variations during summer months, i.e., May to September at the early morning hours from 0600 to 0800 local time and also significant uptake during the day (approx. 0900 local time onwards). Accordingly, the contribution of CH tracer to the diurnal cycle becomes significant during this period.

3.6 *Sensitivity tests for model simulation*

Sensitivity tests have been confined to 5 days in summer (29 July–2 August) and 5 days in winter (16–20 January). While summer situation is presented in figure 9(a, b, c), the corresponding situation in winter is given in figure 9(d, e, f). Two different kinds of sensitivity tests have been performed: (1) by introducing another PBL parameterization scheme, and (2) by increasing the model vertical resolution.

3.6.1 *Impact of changing the boundary layer parameterization scheme*

Two most widely used planetary boundary layer (PBL) parameterization schemes in WRF model version 3.0.1 are Mellor, Yamada and Janjic (MYJ) scheme (Mellor and Yamada 1982; Janjic 1994), and Yonsei University (YSU) scheme (Hong and Kim 2008). Similar sensitivity studies were performed by Gerbig *et al.* (2008), Kretschmer *et al.* (2012) and Lauvaux and Davis (2014). All the groups were interested about the development of mixing height in regional models due to the two different PBL schemes and their error characterization. Our study is confined to the lower height up to 200 m and the vertical gradient of CO_2 concentration. The control simulation has been carried out using MYJ scheme, which is a local 1.5 order turbulence closure scheme. Mellor and Yamada have argued that the scheme is suitable for stable and slightly unstable flows; but, when the flow approaches the free convective limit, transport errors are expected to increase. On the other hand, YSU scheme is a first order non-local scheme with a counter gradient term in eddy diffusion equation.

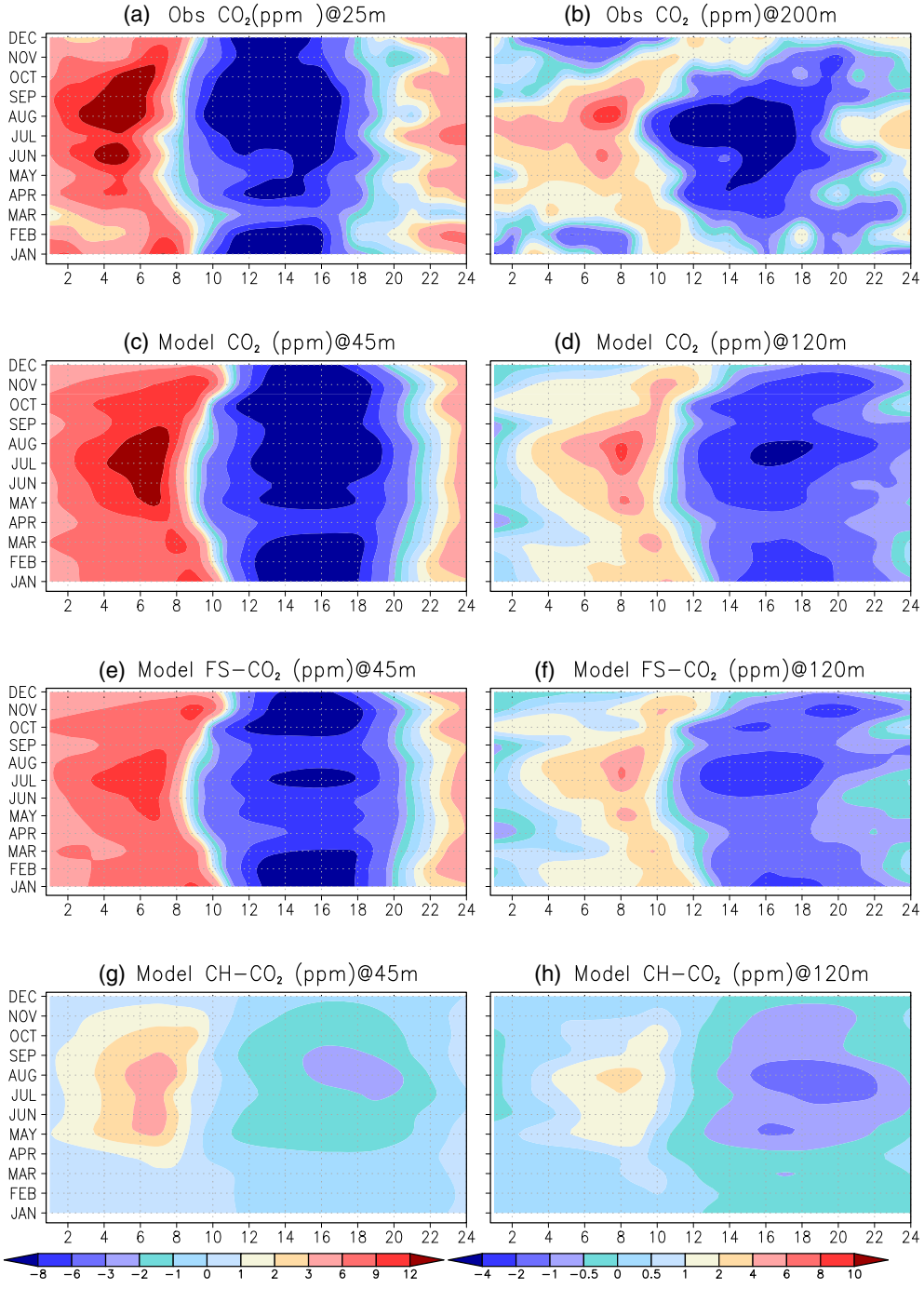

Figure 8. Monthly mean (y-axis) patterns of CO_2 diurnal cycles (x-axis: local time of the day in hour) are depicted for the two different heights in the case of Tsukuba tower. Panels (**a**, **b**) stand for the observed height of 25 and 200 m respectively and panels (**c**, **d**) stand for simulated CO_2 concentration at 45 and 120 m heights, respectively. Panels (**e**, **g**) and (**f**, **h**) stand for FS and CH tracer component contribution respectively at 45 and 120 m heights. Colour bar represents amplitude of CO_2 diurnal cycle in ppm.

When YSU scheme is used in the model with 31 levels (control configuration), the vertical gradient decreases compared to what is noted with MYJ scheme. This occurs both in summer (figure 9a) as well as in winter (figure 9d), showing enhanced mixing in the case of YSU scheme compared to the MYJ scheme (Hu *et al.* 2010; Garcia-Diez *et al.* 2013 and the references therein). The gradients for PM average in two schemes are not much different both in summer as well as winter (figure 9b and e), due to sufficient mixing within the PBL in daytime. But the difference is more pronounced in summer for AM average (figure 9c), when mixing is more pronounced in YSU. In winter, the mixing in the model is more than what is observed and YSU scheme gives excessive mixing (figure 9f). However,

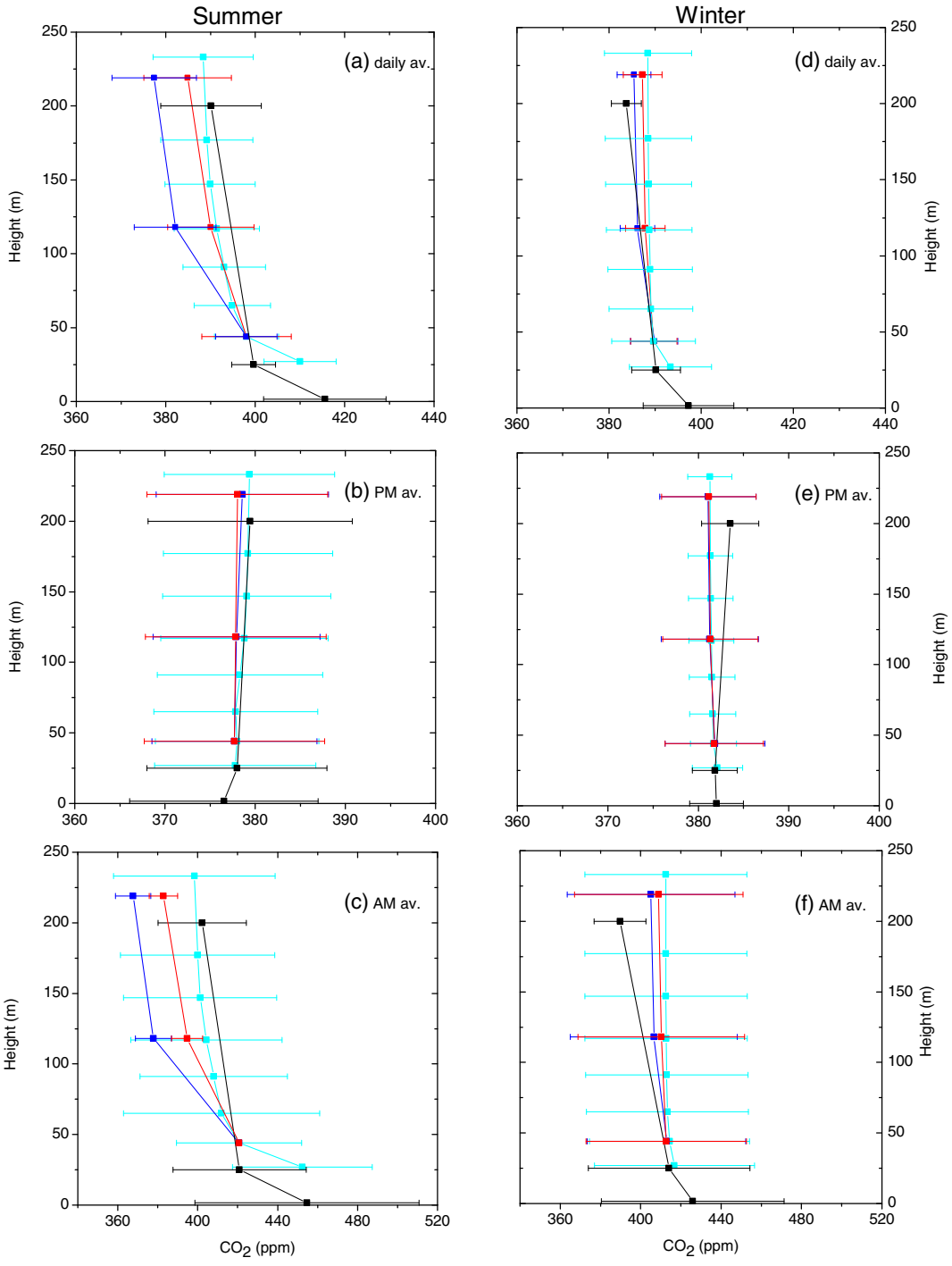

Figure 9. Comparison of measured (black: observation) and simulated (blue: 31 levels MYJ scheme (control case), red: 31 levels YSU scheme, cyan: 37 levels MYJ scheme) vertical profiles of CO_2 concentration at Tsukuba averaged for 5 days in two extreme seasons namely summer (left panel) and winter (right panel). Panels (**a**, **d**), (**b**, **e**) and (**c**, **f**) present daily average, afternoon average (referred as PM; 13 to16 local time) and late night average (referred as AM; 01 to 04 local time) respectively. Standard deviation of 5-day average data is also plotted at each height. Offset of all model results are adjusted at 45 m height with the observed value at 25 m height.

the simulated concentrations using YSU PBL scheme are within the ± 1-σ of the observed concentrations at 200 m. One needs to note that the model fails to simulate the strong gradients in observed CO_2 at the two lower-most levels (1.5 and 25 m for observation, and 45 and 120 m for model) from the earth's surface indicating excessive vertical mixing in the case of YSU scheme.

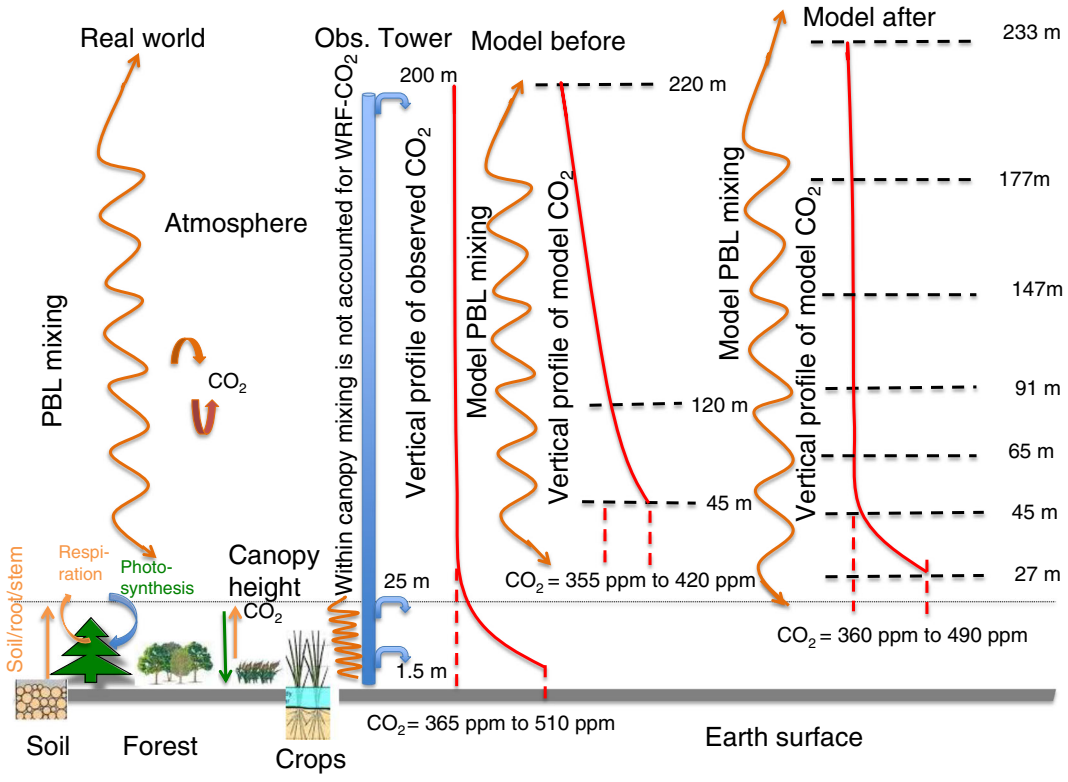

Figure 10. Schematic diagram of futuristic model improvements for simulating observations at tall tower measurements. The grey horizontal bar at the bottom defines the interface between atmosphere and the earth's surface, while the thin black line around 25 m is used for showing the canopy top height. A representative ecosystem distribution and transport mechanism is shown in the left side of the observation tower (blue vertical bar with air intakes at 1.5, 25 and 200 m heights), and the model representation of CO_2 transport in control (center; model before) and finer (right; model after) vertical resolutions are depicted. It is noted that potential CO_2 emission distribution due to soil respiration, heterotrophic respiration and photosynthetic uptake below the canopy top are not represented even in the fine vertical model resolution.

3.6.2 *Impact of increasing the model vertical levels*

As a test case, six more levels have been inserted between the η levels of 1.0 and 0.966 (two levels between 1 and 0.993, three levels between 0.993 and 0.980, and one level between 0.980 and 0.966) of the control model configuration. Now, the lowest model level is located at 27 m from the earth's surface compared to 45 m in the control case. In the increased vertical resolution case (figure 9a, d), the model is able to create strong gradient between the two lowermost levels 27 and 45 m (unlike the YSU PBL scheme). The model also shows vertical CO_2 gradients close to the observed gradients for the heights above 45 m with statistical significance (always within $\pm$1-σ of observed variations). Slight underestimation of simulated CO_2 vertical gradient between 45 and 233 m compared to that between 25 and 200 m for observation during winter is likely to have caused by the lower emissions, as suggested by the weaker simulated gradient between the two lowermost levels. The detailed shape of CO_2 vertical profile between 25 and 200 m is also inconclusive without additional observation levels. This clearly shows improved representation of the tower levels in increased vertical resolution, and particularly highlights the importance of lowering and closely spacing the lowermost levels of the WRF-CO_2 model.

Figure 9(b) (PM average) shows that the drawdown of CO_2 during daytime of summer season in the lowermost region of observation is not as pronounced in the model as the observations due to high vertical mixing in the model or weaker terrestrial biosphere uptake. On the other hand, model and observation profiles match well during the daytime of winter (figure 9e). The pronounced gradients in observed profile during night-time are captured well by the model in both the summer and winter seasons (figure 9c and f).

4. Conclusions and outlook

Concentrations of atmospheric CO_2 are simulated using the Weather Research and Forecasting (WRF-CO_2) model developed at Jadavpur University, in collaboration with RIGC/JAMSTEC. The center of model domain is set at the Kanto plain in Japan, with 132×165 longitude-latitude

grid points of 27 km spacing and 31 vertical levels between the earth's surface and 100 hPa height. Performance of the WRF-CO_2 model has been evaluated using atmospheric CO_2 and meteorological measurements at a tall tower in Tsukuba, Japan, a semi-urban location. Tsukuba is also located close to the mega-city Tokyo with intense fossil fuel emissions. We find, transport variations of fossil fuel emission signal play the most significant role along with the local biospheric sources and sinks during the summer in simulating CO_2 synoptic and diurnal cycle observed at both 25 and 200 m tower heights.

The vertical profile of CO_2 concentration is largely controlled by temperature profile, and net uptake and release of CO_2 during the day and night, respectively. Regional model WRF-CO_2 show significant success in simulation at the surface level, but our analysis reveals limited ability of the model transport in simulating the vertical propagation of the CO_2 flux signals between 25 and 200 m of the tower levels except during the autumn season. This is noted from gradual fall in diurnal cycle and normalized standard deviation of the model simulation from 25 to 145 m and then, to 220 m height. Correlation coefficient shows a significant fall if 220 m of model simulation is compared with 200 m observation height. The simulated vertical gradient in CO_2 concentration also falls at the upper height in all seasons except during autumn.

Mismatches between the simulation and observation resulted due to uncertainties in both model transport and surface fluxes, and their representation errors due to coarse spatial and temporal resolutions. Here, we have run two sets of case studies, namely, the choice of planetary boundary layer (PBL) parameterization scheme and by increasing vertical levels within the PBL. We find that the PBL scheme of Yonsei University mixes CO_2 vertically more readily compared to that of Mellor–Yamada–Janjic, used in our control simulations. However, most dramatic improvement in the WRF-CO_2 simulated vertical gradient is achieved when six vertical levels are inserted between levels 1–4 ($\eta = 1$ and $\eta = 0.966$) of the control model configuration. The cause of this improved vertical simulation is attributed to better representation of the Tsukuba tower levels in the model. The CO_2 gradient between two lowermost model levels at 27 and 45 m are found to be critical for simulating vertical gradients between 25 and 200 m. Measurements at more tower levels between 25 and 200 m are required for diagnosing source of errors WRF-CO_2 simulations.

We have not been able to conduct any sensitivity test of CO_2 simulations for uncertainties in fluxes because of unavailability of the terrestrial biospheric fluxes at finer resolution (presently at $1^\circ \times 1^\circ$ latitude–longitude intervals). There are also limitations on the distribution of the terrestrial biospheric fluxes within the canopy. Presently, the lowest level of WRF-CO_2 simulation is 27 m, which is typically at the top of the canopy, while the tower measurements are made at 1.5, 25 m, and above. Our sensitivity simulation at increased vertical resolution revealed the importance of the lowest two model levels for CO_2 vertical gradients within the PBL. Since, vertical transport of mass is deeply related with fluxes close to surface, assigning terrestrial fluxes from the soil/root, stem and leaf components at appropriate altitudes are essential for further improving the forward model simulations. A schematic diagram of present and futuristic transport model simulation is shown in figure 10. While the WRF-CO_2 simulations improved from the 'before' model to the 'after' model by increasing number of vertical levels from 31 to 37, it must be noted that presently no model framework exists for accounting 3-dimensional canopy structure and thus the distribution of CO_2 sources and sinks, as well as their transport below the canopy top.

The present work has large implication towards the development of future chemistry-transport models and inverse modelling of gases and aerosols. It clearly indicates the necessity of a suitable boundary layer process, increase of model vertical resolution near the surface and to incorporate a canopy model. Chemical tracer observation at more levels close to the surface are also required for validating model transport.

Acknowledgements

SB is supported by a research fellowship award by the Council for Scientific and Industrial Research (CSIR), Government of India. This work is partly supported by JSPS/MEXT KAKENHI-A grant number 22241008. We wish to thank the research teams and support staff of the Tsukuba tall tower observation station for their efforts. Initial support from the GOSAT project and Shamil Maksyutov is greatly appreciated. We acknowledge the help rendered by Dr. Sandipan Mukherjee, GBPIHED, India during the preparation of the manuscript.

References

Ahmadov R, Gerbig C, Kretschmer R, Koerner S, Neininger B, Dolman A J and Sarrat C 2007 Mesoscale covariance of transport and CO_2 fluxes: Evidence from observations and simulations using the WRF-VPRM coupled atmosphere-biosphere model; *J. Geophys. Res.* **112** D22107, doi: 10.1029/2007JD008552.

Bakwin P S, Tans P P, Zhao C, Ussler W I and Quesnell E 1995 Measurements of carbon dioxide on a very tall tower; *Tellus* **47B** 535–549.

Ballav S, Patra P K, Takigawa M, Ghosh S, De U K, Maksyutov S, Murayama S, Mukai H and Hashimoto S 2012 Simulation of CO_2 concentration over east Asia region with the help of the regional model WRF-CO_2; *J. Meteor. Soc. Japan* **90(6)** 959–976.

Corbin K D, Denning A S and Gurney K R 2010 The space and time impacts on U.S. regional atmospheric CO_2 concentrations from a high resolution fossil fuel CO_2 emissions inventory; *Tellus* **62(5)** 506–511.

Denning A, Fung I and Randall D 1995 Latitudinal gradient of atmospheric CO_2 due to seasonal exchange with land biota; *Nature* **376** 240–243.

Freitas S R, Longo K M, Silva Dias M A F, Chatfield R, Silva Dias P, Artaxo P, Andreae M O, Grell G, Rodrigues L F, Fazenda A and Panetta J 2009 The Coupled Aerosol and Tracer Transport model to the Brazilian developments on the Regional Atmospheric Modeling System (CATT-BRAMS) – Part 1: Model description and evaluation; *Atmos. Chem. Phys.* **9** 2843–2861, doi: 10.5194/acp-9-2843-2009.

Garcia-Diez M, Fernandez J, Fita L and Yague C 2013 Seasonal dependence of WRF model biases and sensitivity to PBL schemes over Europe; *Quart. J. Roy. Meteorol. Soc.* **139** 501–514.

Gerbig C, Korner S and Lin J C 2008 Vertical mixing in atmospheric tracer transport models: Error characterization and propagation; *Atmos. Chem. Phys.* **8** 591–602.

Grell G A, Peckham S E, Schmitz R, McKeen S, Frost G, Skamarock W and Eder B 2005 Fully coupled 'online' chemistry within the WRF model; *Atmos. Environ.* **39(37)** 6957–6975.

Haszpra L, Ramonet M, Schmidt M, Barcza Z, Pátkai Zs, Tarczay K, Yver C, Tarniewicz J and Ciais P 2012 Variation of CO_2 mole fraction in the lower free troposphere, in the boundary layer and at the surface; *Atmos. Chem. Phys.* **12** 8865–8875, doi: 10.5194/acp-12-8865-2012.

Hong S-Y and Kim S-W 2008 Stable boundary layer mixing in a vertical diffusion schem; *Proc. Ninth Annual WRF User's Workshop, Boulder, CO, National Center for Atmospheric Research 3.3* [http://www.mmm.ucar.edu/wrf/users/workshops/WS2008/abstracts/3-03.pdf].

Hu X-M, Nielsen-Gammon J W and Zhang F 2010 Evaluation of three planetary boundary layer schemes in the WRF Mode; *J. Appl. Meteorol. Climatol.* **49** 1831–1844.

Inoue H Y and Matsueda H 2001 Measurements of atmospheric CO_2 from a meteorological tower in Tsukuba, Japan; *Tellus* **53(3)** 205–219.

Janjic Z I 1994 The step-mountain Eta coordinate model: Further developments of the convection, viscous layer, and turbulence closure scheme; *Mon. Wea. Rev.* **122** 927–945.

Kretschmer R, Gerbig C, Kartens U and Koch F T 2012 Error characterization of CO_2 vertical mixing in the atmospheric transport model WRF-VPRM; *Atmos. Phys. Chem.* **12** 2441–2458.

Kretschmer R, Gerbig C, Karstens U, Biavati G, Vermeulen A, Vogel F, Hammer S and Totsche K U 2014 Impact of optimized mixing heights on simulated regional atmospheric transport of CO_2; *Atmos. Chem. Phys.* **14** 7149–7172.

Lauvaux T and Davis K J 2014 Planetary boundary layer errors in mesoscale inversions of column-integrated CO_2 measurements; *J. Geophys. Res. Atmos.* **119** 490–508, doi: 10.1002/2013JD020175.

Law R M *et al.* 2008 TransCom model simulations of hourly atmospheric CO_2: Experimental overview and diurnal cycle results for 2002; *Global Biogeochem. Cycles* **22** GB3009, doi: 10.1029/2007GB003050.

Mellor G L and Yamada T 1982 Development of a turbulence closure model for geophysical fluid problem; *Rev. Geophys.* **20** 851–875.

Miles N L, Richardson S J, Davis K J, Lauvaux T, Andrews A E, West T O, Bandaru V and Crosson E R 2012 Large amplitude spatial and temporal gradients in atmospheric boundary layer CO_2 mole fractions detected with a tower-based network in the U.S. upper Midwest; *J. Geophys. Res.* **117** G01019, doi: 10.1029/2011JG001781.

Moreira D S, Freitas S R, Bonatti J P, Mercado L M, Rosário N M E, Longo K M, Miller J B, Gloor M and Gatti L V 2013 Coupling between the JULES land-surface scheme and the CCATT-BRAMS atmospheric chemistry model (JULES-CCATT-BRAMS1.0): Applications to numerical weather forecasting and the CO_2 budget in South America; *Geosci. Model Dev.* **6** 1243–1259.

Nakazawa T, Ishizawa M, Higuchi K and Travett N B A 1997 Two curve fitting methods applied to CO_2 flask data; *Environmetrics* **8** 197–218.

Olivier J G J and Berdowski J J M 2001 Global emission sources and sinks; In: *The Climate System* (eds) Berdowski, J, Guicherit R and Heij B J, Balkema A A, Lisse, Netherlands, pp. 33–78, ISBN: 9058092550.

Olsen S C and Randerson J T 2004 Differences between surface and column atmospheric CO_2 and implications for carbon cycle research; *J. Geophys. Res.* **109** D02301, doi: 10.1029/2003JD003968.

Palmiéri J, Orr J C, Dutay J-C, Béranger K, Schneider A, Beuvier J and Somot S 2015 Simulated anthropogenic CO_2 storage and acidification of the Mediterranean Sea; *Biogeosci.* **12** 781–802.

Patra P K and Law R M *et al.* 2008 TransCom model simulations of hourly atmospheric CO_2: Analysis of synoptic-scale variations for the period 2002–2003; *Global Biogeochem. Cycles* **22** GB4013, doi: 10.1029/2007GB003081.

Peylin P, Houweling S, Krol M C, Karstens U, Rödenbeck C, Geels C, Vermeulen A, Badawy B, Aulagnier C, Pregger T, Delage F, Pieterse G, Ciais P and Heimann M 2011 Importance of fossil fuel emission uncertainties over Europe for CO_2 modelling: Model intercomparison; *Atmos. Chem. Phys.* **11** 6607–6622, doi: 10.5194/acp-11-6607-2011.

Pillai D, Gerbig C, Ahmadov R, Roedenbeck C, Kretschmer R, Koch T, Thompson R, Neininger B and Lavric J V 2011 High-resolution simulations of atmospheric CO_2 over complex terrain – representing the Ochsenkopf mountain tall tower; *Atmos. Chem. Phys.* **11** 7445–7464, doi: 10.5194/acp-11-7445-2011.

Sarrat C, Noilhan J, Lacarrére P, Ceschia E, Ciais P, Dolman A J, Elbers J A, Gerbig C, Gioli B, Lauvaux T, Miglietta F, Neininger B, Ramonet M, Vellinga O and Bonnefond J M 2009 Mesoscale modelling of the CO_2 interactions between the surface and the atmosphere applied to the April 2007 CERES field experiment; *Biogeosci.* **6** 633–646.

Smallman T L, Williams M and Moncrieff J B 2014 Can seasonal and interannual variation in landscape CO_2 fluxes be detected by atmospheric observation of CO_2 concentrations made at tall tower?; *Biogeosci.* **11** 735–747.

Seibert P, Beyrich F, Gryning S-E, Joffre S, Rasmussen A and Tercier Ph 1998 Mixing height determination for dispersion modelling, Report of Working Group 2; In: Harmonization in the preprocessing of meteorological data for atmospheric dispersion models; *COST Action 710, CEC Publication EUR* **18195** 145–265.

Takahashi T, Sutherland S C, Sweeney C and Poisson A *et al.* 2002 Global sea–air CO_2 flux based on climatological surface ocean pCO_2, and seasonal biological and temperature effects; *Deep Sea Res.: Part II* **49** 1601–1622, doi: 10.1016/S0967-0645(02)00003-6.

Takigawa M, Niwano M, Akimoto H and Takahashi M 2007 Development of a one-way nested global-regional air quality forecasting model; *SOLA* **3** 81–84, doi: 10.2151/sola.2007-021.

Tolk L F, Meesters A G C A, Dolman A J and Peters W 2008 Modelling representation errors of atmospheric CO_2 mixing ratios at a regional scale; *Atmos. Chem. Phys.* **8** 6587–6596.

Tolk L F, Dolman A J, Meesters A G C A and Peters W 2011 A comparison of different inverse carbon flux estimation approaches for application on a regional domain; *Atmos. Chem. Phys.* **11** 10349–10365.

Vogel F R, Thiruchittampalam B, Theloke J, Kretschmer R, Gerbig C, Hammer S and Levin I 2013 Can we evaluate a fine-grained emission model using high-resolution atmospheric transport modelling and regional fossil fuel CO_2 observations?; *Tellus B* **65** 18681.

MS received 16 April 2015; revised 13 August 2015; accepted 4 September 2015